KnE Energy & Physics

ICPPA 2017
The 3rd International Conference on Particle Physics and Astrophysics
Volume 2018

Knowledge E
Engaging minds

Conference Paper

# Review of the theoretical heavy-ion physics

## E. L. Bratkovskaya[1,3], W Cassing[2], P. Moreau[3], and T. Song[2]

[1]GSI Helmholtzzentrum für Schwerionenforschung GmbH, Darmstadt, Germany
[2]Institute for Theoretical Physics, University of Giessen, Giessen, Germany
[3]Institute for Theoretical Physics, University of Frankfurt, Frankfurt, Germany

## Abstract

In this contribution we briefly give an overview of the theoretical models used to describe experimental data from heavy-ion collisions from $\sqrt{s_{NN}} \approx 4$ GeV to ultra-relativistic energies of $\sqrt{s_{NN}} \approx 5$ TeV. We highlight the successes and problems of statistical or hadron-resonance gas models, address the results of macroscopic approaches like hydrodynamics (in different hybrid combinations) as well as the results from microscopic transport approaches in comparison to experimental data. Finally, the transport coefficients like shear $\eta$ and bulk viscosity $\zeta$ - entering the macroscopic models - are confronted with results from lattice QCD in thermal equilibrium for vanishing chemical potential.

Corresponding Author:
E. L. Bratkovskaya
E.Bratkovskaya@gsi.de

## 1. Introduction

The dynamics of the early universe in terms of the 'Big Bang' may be studied experimentally by relativistic nucleus-nucleus collisions from Alternating Gradient Synchrotron (AGS) to Large-Hadron-Collider (LHC) energies in terms of 'tiny bangs' in the laboratory. With sufficiently strong parton interactions, the medium in the collision zone can be expected to achieve local equilibrium after some initial delay and exhibit approximately hydrodynamic flow [1–3]. In these collisions a new state of strongly interacting matter is created, being characterized by a very low shear viscosity $\eta$ to entropy density $s$ ratio, $\eta/s$, close to a nearly perfect fluid [4, 5]. Lattice QCD (lQCD) calculations [6, 7] indicate that a crossover region between hadron and quark-gluon matter should have been reached in these experiments (at least at higher energies). Apart from a deconfinement transition also a restoration of chiral symmetry should occur at about the same critical temperature in case of vanishing baryon chemical potential. Whereas at low chemical potential the transition is known to be a crossover [8, 9] it is presently unclear if there will be a critical point in the QCD phase diagram marking the transition to a first-order domain [10]. Furthermore, it is doubted that the restoration of chiral symmetry and the deconfinement transition will happen

How to cite this article: E. L. Bratkovskaya, W Cassing, P. Moreau, and T. Song, (2018), "Review of the theoretical heavy-ion physics" in *The 3rd International Conference on Particle Physics and Astrophysics*, KnE Energy & Physics, pages 234–246. DOI 10.18502/ken.v3i1.1749

Page 234

at the same point in the phase diagram once high baryon chemical potentials are encountered [11–13]. This situation will be met experimentally in heavy-ion collisions at FAIR/NICA energies in the future [14].

Since the hot and dense matter produced in relativistic heavy-ion collisions appears only for a couple of fm/c, it is a challenge for experiment to investigate its properties. The differential spectra of hadrons with light quarks/antiquarks provide information about the bulk dynamics whereas abundances and differential spectra of hadrons with strange/antistrange quarks shed light on the chemical equilibration processes. Furthermore, the electromagnetic emissivity of the matter produced in heavy-ion collisions is tested by direct photon spectra as well as dileptons which might provide additional information on the properties of vector resonances in a dense hadronic medium. Also the heavy flavor mesons are considered to be promising probes since the production of heavy flavor requires a large energy-momentum transfer and takes place early in the heavy-ion collisions, and - due to the large energy-momentum transfer - should be described by perturbative quantum chromodynamics (pQCD). The produced heavy flavor then interacts with the hot dense matter (of partonic or hadronic nature) by exchanging energy and momentum which is controlled by a spatial diffusion constant $D_s(T, \mu_B)$. Let's have a brief look at the various model concepts.

# 2. Statistical, macroscopic and microscopic models

## 2.1. Hadron resonance gas (HRG) or statistical models

In case of very strong interactions of the degrees of freedom in the collision zone of relativistic heavy-ion collisions one might infer that a thermal and chemical equilibrium has been achieved (at least at freezeout) and the final hadronic spectra can be described by a grand-canonical ensemble assuming the conservation of energy, particle number and volume on average. When looking at particle ratios the volume drops out - implying similar freezeout conditions and collective flow for all hadrons - and one is left with essentially two Lagrange parameters that are attributed to a temperature $T$ and baryon chemical potential $\mu_B$. Thus - looking at central collisions of Au+Au (Pb+Pb) - one can extract a freezeout line in the QCD phase diagram by fitting the measured particle ratios (dominantly at midrapidity) at different bombarding energies. In fact, the results of such fits are in a good agreement with experimental observation from AGS to top LHC energies [15, 16] over many orders of magnitude once some parameter for the excluded volume of hadrons ($r_0 \approx 0.3$ fm) is chosen

properly in order to reduce the net density. Especially at top LHC energies only a single parameter $T$ survives since $\mu_B \approx 0$. In principle the inclusion of resonances is akin to an interacting theory of 'fundamental' hadrons with attractive interactions; the concept of an excluded volume decreases the density and increases the pressure thus simulating additional repulsive interactions. These models are reminiscent of Van der Waals gases and recent statistical models actually are formulated along this line or incorporate explicit baryon-baryon interactions [17–19]. Accordingly, the formulation of interacting hadron resonance gas models (IHRG) will provide a link between the actual interaction parameters and fundamental many-body theories (e.g. Brueckner) or $S$-matrix approaches.

However, the question about the dynamics of equilibration and the generation of collective flow in heavy-ion collisions remains open in the HRG or IHRG approaches. Furthermore, the evaluation of photon or dilepton spectra cannot be addressed in the grandcanonical (or canonical) models since the real and virtual photons are not in equilibrium with their environment due to the low electromagnetic coupling ($\alpha_e \approx 1/137$). Some of these questions, however, can be addressed in macroscopic models.

## 2.2. Hydro and hybrid models

In order to obtain some information on the space-time dynamics of heavy-ion collisions one often employs hydrodynamical models which are of one-fluid [2] or three-fluid [20] nature. In the one-fluid models the initial conditions for the hydro-evolution (at some finite time $t_0$ assumed for local equilibration) are essentially fixed by the final hadron spectra and the generation of collective flow in the fluid follows from the local pressure gradients (adopting some equation of state (EoS) for the fluid). In this case one can model various EoS relating to a hadronic one, to lattice QCD or a model EoS with a first order phase transition in order to test the sensitivity of observables like collective flow coefficients $v_n$ ($n$=1,2,3,4,..) as a function of bombarding energy and centrality of the collision. However, in ideal hydrodynamical simulations it was found that the elliptic flow as a function of transverse momentum $v_2(p_T)$ was overestimated in comparison to experimental data at RHIC thus signalling a finite shear viscosity $\eta$. Actually, there is a lower limit on the ratio of shear viscosity over entropy density $\eta/s \geq 1/(4\pi)$ [21] such that viscous hydrodynamics had to be employed [22]. Furthermore, also a finite (and even large) bulk viscosity $\zeta(T)$ for temperatures close to $T_c \approx 158$ MeV should be incorporated. With the appearance of two additional transport coefficients $\eta(T)$ and $\zeta(T)$ one had to specify their functional form since results from

pQCD turned out to be fully misleading. On the other hand a significant triangular flow $v_3(p_T)$ demonstrated the importance of initial-state fluctuations that had to be incorporated in the initial conditions of the hydro phase [23]. Furthermore, resonant hadronic scattering - after chemical freezeout - had to be included since the hadrons still keep interacting after chemical freezeout [24]. This lead to the development of hybrid models which incorporate three different type of model components:

- i) the initial nonequilibrium phase to specify the initial state fluctuations or initial flow
- ii) viscous hydro for the partonic (fluid) phase
- iii) hadronic 'afterburner' for resonant interactions in the hadronic phase after freezeout.

Due to the matching of the different phases a couple of new parameters enter such models that define the matching conditions. Accordingly, a multi-parameter approach (on the scale of $\sim$ 15 independent parameters) emerges that has to be optimized in comparison to a multitude of experimental data in order to extract physical information on the transport coefficients. This has been done within a Bayesian analysis by a couple of authors and some proper information could be extracted so far on $\eta/s(T)$ as well as for the charm diffusion coefficient $D_s(T)$ [25–27]. For explicit results we refer the reader to Refs. [25–31]. We note in passing that within such approaches semi-central and central nucleus-nucleus collisions at ultra-relativistic energies can well be described [32] but an application to elementary high-energy $p + p$ or $\pi + p$ reactions is difficult/questionable.

In this class of models we mention also the ultra-relativistic quantum molecular dynamics (UrQMD) hybrid approach which starts with UrQMD [33] for the initial nonequilibrium phase on an event by event basis, switches to hydro after approximate equilibration in local cells of higher energy density, continues with a hydro evolution until freezeout (at equal times) and follows with UrQMD to describe the final hadronic rescatterings [34]. By construction such hybrid models may be used for lower (AGS) energies as well as for ultra-relativistic (LHC) energies. A systematic study of transport properties in the fluid phase is still not available so far. Further attempts incorporating a color glass condensate (CGC) for the initial conditions, IP-glasma or EPOS2 initial conditions [35–41] provide also a good description of the collective flows as a function of bombarding energy and collision centrality at RHIC and LHC energies.

A further advantage of hydro or hybrid models is that one can calculate the differential photon and dilepton production by integration of microscopic production rates

in space and time [42, 43]. Especially in the partonic phase the AMY rates [44] are employed for photon production by most of the authors whereas the evolution of the electromagnetic emissivity in the hadronic phase differs substantially within the different variants.

## 2.3. Microscopic transport models

Whereas early microscopic transport models have been developed for the dynamics of hadrons employing a nuclear matter EoS and cross sections based on experimental data or effective hadronic Lagrangians [45–47] later versions have included the formation and decay of strings [33, 48, 49] to incorporate multi-particle production with increasing energy which becomes essential at AGS and SPS energies. However, when applied to heavy-ion collisions at RHIC energies a couple of problems emerged since a number of observables (elliptic flow of charged hadrons, transverse mass spectra of hadrons, intermediate mass dileptons etc.) could no longer be properly described by hadron-string degrees of freedom [50, 51]. This lead to the formulation of transport models for partonic degrees of freedom of Boltzmann-type that were first based on pQCD based cross sections [52, 53] with an ideal gas EoS for the partonic phase. Since pQCD scattering cross sections between massless partons turned out too low in order to describe the elliptic flow of hadrons measured experimentally, either effective (enhanced) two-body cross sections have been used [54] or additional $2 \leftrightarrow 3$ channels have been added as in BAMPS [53]. The formation of hadrons is usually performed by coalescence either in momentum space or - more recently - in phase space. Another branch of transport models is based on NJL-like approaches including a coupling to a scalar mean field and/or a vector mean field [55, 56]. In these models the partons have a finite dynamical mass and the binary cross sections are either extracted from the NJL Lagrangian [56] or parameterized to simulate a finite $\eta/s$ (as in hydro models) [57]. All these approaches provide a reasonable description of experimental data at RHIC energies as well as for LHC energies.

The Parton-Hadron-String Dynamics (PHSD) transport approach [58, 59] is a microscopic covariant dynamical model for strongly interacting systems formulated on the basis of Kadanoff-Baym equations [60] for Green's functions in phase-space representation (in first order gradient expansion beyond the quasiparticle approximation). The approach consistently describes the full evolution of a relativistic heavy-ion collision from the initial hard scatterings and string formation through the dynamical deconfinement phase transition to the strongly-interacting quark-gluon plasma (sQGP) as well as

hadronization and the subsequent interactions in the expanding hadronic phase as in the Hadron-String-Dynamics (HSD) transport approach [48]. The transport theoretical description of quarks and gluons in the PHSD is based on the Dynamical Quasi-Particle Model (DQPM) for partons that is constructed to reproduce lQCD results for a quark-gluon plasma in thermodynamic equilibrium [60] on the basis of effective propagators for quarks and gluons. The DQPM is thermodynamically consistent and the effective parton propagators incorporate finite masses (scalar mean-fields) for gluons/quarks as well as a finite width that describes the medium dependent reaction rate. For fixed thermodynamic temperature $T$ the partonic width's $\Gamma_i(T)$ fix the effective two-body interactions that are presently implemented in the PHSD [61]. The PHSD differs from conventional Boltzmann approaches in a couple of essential aspects:

- it incorporates dynamical quasi-particles due to the finite width of the spectral functions (imaginary part of the propagators) in line with complex retarded self-energies;

- it involves scalar mean-fields that substantially drive the collective flow in the partonic phase;

- it is based on a realistic equation of state from lattice QCD and thus reproduces the speed of sound $c_s(T)$ reliably;

- the hadronization is described by the fusion of off-shell partons to off-shell hadronic states (resonances or strings);

- all conservation laws (energy-momentum, flavor currents etc.) are fulfilled in the hadronization contrary to coalescence models;

- the effective partonic cross sections no longer are given by pQCD and are 'defined' by the DQPM in a consistent fashion. These cross sections are probed by transport coefficients (correlators) in thermodynamic equilibrium by performing PHSD calculations in a finite box with periodic boundary conditions (shear- and bulk viscosity, electric conductivity, magnetic susceptibility etc. [62, 63]).

The transition from the partonic to hadronic degrees-of-freedom (for light quarks/antiquarks) is described by covariant transition rates for the fusion of quark-antiquark pairs to mesonic resonances or three quarks (antiquarks) to baryonic states, i.e. by the dynamical hadronization [58]. Note that due to the off-shell nature of both partons and hadrons, the hadronization process described above obeys all conservation laws (i.e. four-momentum conservation and flavor current conservation) in each event, the detailed balance relations and the increase in the total entropy $S$. In the hadronic phase PHSD is equivalent to the hadron-strings dynamics (HSD) model [48] that has been

employed in the past from SIS to SPS energies. On the other hand the PHSD approach has been tested for p+p, p+A and relativistic heavy-ion collisions from lower SPS to LHC energies and been successful in describing a large number of experimental data including single-particle spectra, collective flow [59] as well as electromagnetic probes [64] or charm observables [65, 66].

Apart from deconfinement the chiral symmetry restoration (CSR) addresses another aspect of the QCD phase diagram in the $(T, \mu_B)$-plane as an additional transition between a phase with broken and a phase with restored chiral symmetry. As in case of the QCD deconfinement phase transition, the boundaries of the CSR phase transition line are not well known. Lattice QCD (lQCD) calculations show that at vanishing baryon chemical potential $\mu_B$=0 the CSR takes place at roughly the same critical temperature and energy density as the deconfinement phase transition which is a crossover. At finite baryon chemical potential lQCD calculations cannot be performed due to the sign problem and one must rely on effective models (or extrapolations) in order to study the QCD phase transitions [14]. Different models support the idea that at finite chemical potential a partially restored phase is achieved before the deconfinement occurs [11, 12]. In order to distinguish the two phases of such a transition, effective models use the scalar quark condensate $\langle \bar{q}q \rangle$ as an order parameter. As the baryon density and temperature increase, the scalar quark condensate $\langle \bar{q}q \rangle$ is expected to decrease from a non-vanishing value in the vacuum to $\langle \bar{q}q \rangle \approx 0$ which corresponds to CSR. Since $\langle \bar{q}q \rangle$ is not a measurable quantity, it is crucial to determine experimental observables which are sensitive to this quantity. Since long the dilepton spectroscopy has been in the focus in this respect since in a chirally restored phase the spectral functions of the the $\rho$- and the $a_1$-meson should become identical. However, no clear evidence has been achieved so far [67]. On the other hand, the enhanced strangeness production at AGS and lower SPS energies was found to be a signature of CSR [68, 69] within the PHSD approach where the local scalar quark condensate was evaluated along the line of the Hellmann-Feynman theorem from the scalar density of hadrons (cf. Ref. [69] for details).

Accordingly, microscopic transport approaches provide a bridge from $p + p$, to $p + A$ and $A + A$ collisions and allow for a transparent interpretation of differential particle spectra, collective flow and electromagnetic observables from experimental studies at various facilities and a wide energy range. Open problems are still many-body reactions - except for $2 \leftrightarrow 3$ channels [70, 71] - and the dynamical modeling of first-order transitions in transport. The formation of clusters is still a task to be solved as well as the inclusion of chiral anomalies.

## 3. Transport coefficients

Information on the QCD phase diagram from strongly interacting matter does not only come from experimental studies but can also be addressed by *ab initio* QCD calculations on a discrete (Euklidean) space-time lattice. Due to the Fermion-sign problem direct lQCD calculations cannot be performed at finite chemical potential, however, valuable information can be inferred from lQCD calculations at imaginary chemical potentials as well as by Taylor expansions. Here the second order expansion coefficients - related to susceptibilities as e.g. $\chi_B = \partial^2 P/\partial\mu_B^2$ - can be evaluated at vanishing $\mu_B$ and provide a first glance in $\mu_B$ direction at finite temperature $T$. Here $P$ denotes the pressure which is identical to the (negative) grand-canonical partition function. Apart from susceptibilities $\chi_x$ also transport coefficients (shear viscosity $\eta(T)$, bulk viscosity $\zeta(T)$, electric conductivity $\sigma_e(T)$, spatial diffusion constant $D_s(T)$ for charm quarks etc.) can be calculated on the lattice although with still quite some uncertainties. These transport coefficients either enter the viscous hydro calculations (Section 2.2) as input or can be confronted with the Bayesian results from hydro (or hybrid) calculations in comparison to a large set of different observables (cf. Section 2.2).

On the other hand, the microscopic transport models can be studied also in a finite box at some initial energy density $\epsilon$ and net-particle number density $n_B$ employing periodic boundary conditions. Within the Kubo formalism [72] or the relaxation-time approximation (RTA) [73] then the transport coefficients can be determined in equilibrium (after some finite equilibration time to determine the thermodynamic variables $T$ and $\mu_B$) and be confronted with results from lQCD. Since in leading order the relation between pressure $P$ and energy density $\epsilon$ is relevant or in particular the speed of sound squared $c_s^2(T) = \partial P/\partial\epsilon$, the microscopic transport models, that claim to describe experimental data, also have to reproduce $c_s^2(T)$ to provide a consistent picture. This excludes those models with massless weakly interacting partons since the EoS cannot be reproduced in the vicinity of the critical temperature $T_c$. We note in passing that explicit comparisons of both methods (Kubo and RTA) in Ref. [61] for $\eta/s$ have shown that the solutions are rather close. This holds especially for the case of the scattering of massive partons where the transport cross section is not very different from the total cross section as also pointed out in Ref. [74].

In Fig. 1 we display different results for $\eta/s$ (a) and $\zeta/s$ versus the scaled temperature $T/T_c$. All variants suggest that $\eta/s$ has a minimum close to $T_c$ whereas $\zeta/s$ shows a maximum close to $T_c$. It is worth noting that especially for the shear viscosity the results from PHSD simulations from the relaxation-time approximation (red line + diamonds)
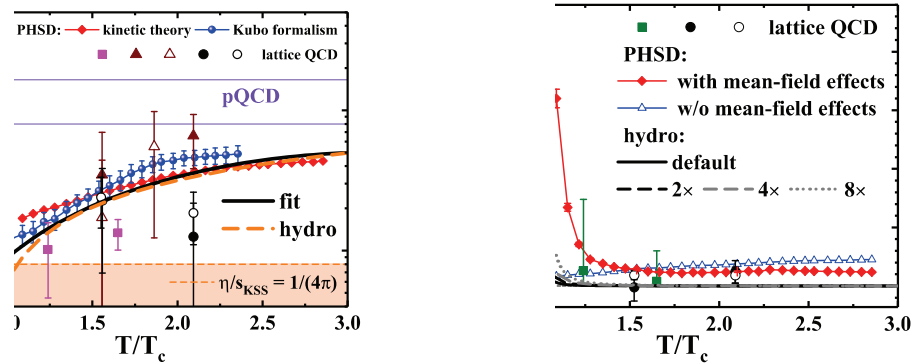
**Figure** 1: $\eta/s$ (a) and $\zeta/s$ versus scaled temperature $T/T_c$.(a) The symbols indicate the PHSD results of $\eta/s$ from Ref. [61], calculated using different methods: the relaxation-time approximation (red line + diamonds) and the Kubo formalism (blue line + dots); the black line corresponds to the parametrization of the PHSD results for $\eta/s$. The orange short dashed line demonstrates the Kovtun-Son-Starinets bound [21] $(\eta/s)_{KSS} = 1/(4\pi)$. The orange dashed line is the $\eta/s$ of the VISHNU hydrodynamical model that was recently determined by a Bayesian analysis. (b) $\zeta/s$ from PHSD simulations from Ref. [61] and the $\zeta/s$ adapted in the hydrodynamical simulations of Ref. [75]. The symbols with (large) error bars are lQCD results from different groups. The figures are taken from Ref. [75].

and the Kubo formalism (blue line + dots) are in close agreement with those from the Bayesian analysis within the VISHNU hydrodynamical model (orange dashed line) as well as with the results from lQCD. This demonstrates that the different theoretical methods outlined above come to approximately the same answers.

## 4. Summary

In this contribution we have briefly discussed the various models used for the description of observables from relativistic heavy-ion collisions in the energy range from the AGS to the LHC and pointed out their successes, range of applications and problems. Whereas statistical models provide no dynamical information the hydro or hybrid models need external information with respect to the transport coefficients and initial conditions/fluctuations. These models succeed in describing various phenomena of relativistic heavy-ion collisions and a Bayesian analysis of a large set of experimental data allows to pin down constraints on the transport coefficients of interest. On the other hand, microscopic transport models provide a bridge from $p + p$, to $p + A$ and $A+A$ collisions and allow for a transparent interpretation of differential particle spectra, collective flow and electromagnetic observables from experimental studies at various facilities and a wide energy range. It is interesting to note that different methods have almost converged to the same results for the shear viscosity (cf. Fig. 1) which demonstrates that complementary strategies lead to a closer physical understanding of the strongly interacting matter produced in heavy-ion reactions. Open problems in

microscopic transport approaches are still many-body reactions, the dynamical modeling of first-order transitions, the formation of clusters as well as the inclusion of chiral anomalies.

## Acknowledgements

## References

 [1] Ollitrault J Y 1992 *Phys. Rev.* D **46** 229

 [2] Heinz U and Kolb P 2002 *Nucl. Phys.* A **702** 269

 [3] Shuryak E V 2009 *Prog. Part. Nucl. Phys.* **62** 48

 [4] Shuryak E V 2005 *Nucl. Phys.* A **750** 64

 [5] Gyulassy M and McLerran L 2005 *Nucl. Phys.* A **750** 30

 [6] Cheng M *et al.* 2008 *Phys. Rev.* D **77** 014511

 [7] Aoki Y *et al.* 2009 *JHEP* **0906** 088

 [8] Borsanyi S Fodor Z Hoelbling C Katz S D Krieg S Szabo K K 2014 *Phys. Lett.* B **730** 99

 [9] Karsch F 2013 *PoS* **CPOD2013** 046

[10] Luo X and Xu N 2017 *Nucl. Sci. Tech.* **28** 112

[11] McLerran L Pisarski R D 2007 *Nucl. Phys.* A **796** 83

[12] Andronic A *et al.* 2010 *Nucl. Phys.* A **837** 65

[13] Fukushimi K Sasaki C 2013 *Prog. Part. Nucl. Phys.* **72** 99

[14] Senger P *et al.* 2011 *Lect. Notes Phys.* **814** 681

[15] Andronic A *et al.* 2016 *Eur. Phys. J.* C **76** 107

[16] Andronic A Braun-Munzinger P Redlich K Stachel J 2017 *arXiv:1710.09425*

[17] Poberezhnyuk R V Vovchenko V Anchishkin D V Gorenstein M I 2017 *arXiv:1708.05605*

[18] Vovchenko V *et al.* 2017 *Phys. Rev.* C **96** 045202

[19] Vovchenko V *et al.* 2017 *Phys. Rev. Lett.* **118** 182301

[20] Ivanov Y B Russkikh V N Toneev V D 2006 *Phys. Rev.* C **73** 044904
     Ivanov Y B Blaschke D 2015 *Phys. Rev.* C **92** 024916

[21] Kovtun P Son D T Starinets A O 2005 *Phys. Rev. Lett.* 94 111601

[22] Jeon S Schenke B 2013 *Int. J. Mod. Phys.* A **28** 1340011

[23] Schenke B Jeon S Gale C 2011 *Phys. Rev. Lett.* **106** 042301

[24] Steinheimer J Aichelin J Bleicher M Stöcker H 2017 *Phys. Rev. C* **95** 064902

[25] Bass S A Bernhard J E Moreland J S 2017 *Nucl.Phys.* A **967** 67

[26] Karpenko I Bernhard J E Bass S A 2017 *arXiv:1706.03666*

[27] Xu Y Nahrgang M Cao S Bernhard J E Bass S A 2017 *arXiv:1710.00807*

[28] Bernhard J E Moreland J S Bass S A Liu J Heinz U 2016 *Phys.Rev. C* **94** 024907

[29] Pratt S Young C 2017 *Phys. Rev. C* **95** 054901

[30] Sangaline E Pratt S 2016 *Phys. Rev. C* **93** 024908

[31] Pratt S Sangaline E Sorensen P Wang H 2015 *Phys. Rev. Lett.* **114** 202301

[32] Song H Bass S A Heinz U W 2014 *Phys.Rev. C* **89** 034919

[33] Bass S A *et al.* 1998 *Prog. Part. Nucl. Phys.* **42** 279

[34] Petersen H *et al.* 2008 *Phys. Rev. C* **78** 044901

[35] Schenke B Schlichting S 2016 *Phys. Rev. C* **94** 044907

[36] Gelis F Schenke B 2016 *Ann. Rev. Nucl. Part. Sci.* **66** 73

[37] Schenke B Tribedy P Venugopalan R 2012 *Phys. Rev. Lett.* 108 252301

[38] Schenke B Tribedy P Venugopalan R 2014 *Nucl. Phys.* A 931 288

[39] Werner K Karpenko I Pierog T Bleicher M Mikhailov K 2010 *Phys. Rev. C* **82** 044904

[40] Werner K Karpenko I Bleicher M Pierog T Porteboeuf-Houssais S 2012 *Phys. Rev. C* **85** 064907

[41] Nahrgang M Aichelin J Bass S Gossiaux P B Werner K 2014 *Nucl. Phys.* A **931** 575

[42] van Hees H Gale C Rapp R 2011 *Phys. Rev. C* **84** 054906

[43] Paquet J F *et al.* 2016 *Phys. Rev. C* **93** 044906

[44] Arnold P B Moore G D Yaffe L G 2001 *JHEP* **0112** 009

[45] Cassing W Metag V Mosel U Niita K 1990 *Phys. Rep.* **188** 363

[46] Hartnack C *et al.* 1998 *Eur. Phys. J. A* **1** 151

[47] Larionov A B Cassing W Greiner C Mosel U 2000 *Phys.Rev. C* **62** 064611

[48] Cassing W Bratkovskaya E L 1999 *Phys. Rep.* **308** 65

[49] Ehehalt W Cassing W 1996 *Nucl. Phys.* A **602** 449

[50] Bratkovskaya E L *et al.* 2004 *Phys. Rev. C* **69** 054907

[51] Bratkovskaya E L Soff S Stöcker H van Leeuwen M Cassing W 2004 *Phys. Rev. Lett.* **92** 032302

[52] Lin Z W *et al.* 2005 *Phys. Rev. C* **72** 064901

[53] Xu Z and Greiner C 2005 *Phys. Rev.* C **71** 064901

[54] Ko C M Song T Li F Greco V Plumari S 2014 *Nucl.Phys.* A **928** 234

[55] Ruggieri M Scardina F Plumari S Greco V 2013 *Phys. Lett.* B **727** 177

[56] Marty R Aichelin J 2013 *Phys. Rev.* C **87** 034912

[57] Ruggieri M Scardina F Plumari S Greco V 2014 *Phys. Rev.* C **89** 054914

[58] Cassing W Bratkovskaya E L 2009 *Nucl. Phys.* A **831** 215
Bratkovskaya E L *et al.* 2011 *Nucl. Phys.* A **856** 162

[59] Linnyk O Bratkovskaya E Cassing W 2016 *Prog. Part. Nucl. Phys.* **87** 50

[60] Cassing W 2009 *Eur. Phys. J. ST* **168** 3

[61] Ozvenchuk V Linnyk O Gorenstein M I Bratkovskaya E L Cassing W 2013 *Phys. Rev.* C **87** 024901

[62] Ozvenchuk V Linnyk O Gorenstein M I Bratkovskaya E L Cassing W 2013 *Phys. Rev.* C **87** 064903

[63] Cassing W Linnyk O Steinert T Ozvenchuk V 2013 *Phys. Rev. Lett.* **110** 182301
Steinert T Cassing W 2014 *Phys. Rev.* C **89** 035203

[64] Linnyk O Cassing W and Bratkovskaya E L 2014 *Phys.Rev.* C **89** 034908
Linnyk O Konchakovski V P Cassing W and Bratkovskaya E L 2013 *Phys. Rev.* C **88** 034904
Linnyk O Konchakovski V Steinert T Cassing W Bratkovskaya E L 2015 *Phys. Rev.* C **92** 054914

[65] Song T Berrehrah H Cabrera D Torres-Rincon J M Tolos L Cassing W Bratkovskaya E 2015 *Phys. Rev.* C **92** 014910

[66] Song T Berrehrah H Cabrera D Cassing W Bratkovskaya E 2016 *Phys. Rev.* C **93** 034906

[67] Rapp R 2013 *Adv. High Energy Phys.* **2013** 148253
Rapp R 2013 *J. Phys. Conf. Ser.* **420** 012017

[68] Cassing W Palmese A Moreau P Bratkovskaya E L 2016 *Phys. Rev.* C **93** 014902

[69] Palmese A Cassing W Seifert E Steinert T Moreau P Bratkovskaya E L 2016 *Phys. Rev.* C **94** 044912

[70] Cassing W 2002 *Nucl. Phys.* A **700** 618

[71] Seifert E Cassing W 2017 *arXiv:1710.00665*

[72] Kubo R 1957 *J. Phys. Soc. Jpn.* **12** 570
Kubo R 1957 *Rep. Prog. Phys.* **29** 255

[73] Chakraborty P Kapusta J I 2011 *Phys. Rev.* **C83** 014906

[74] Plumari S Puglisi A Scardina F Greco V 2012 *Phys. Rev.* C **86** 054902

[75] Xu Y *et al.* 2017 *Phys. Rev.* C **96** 024902